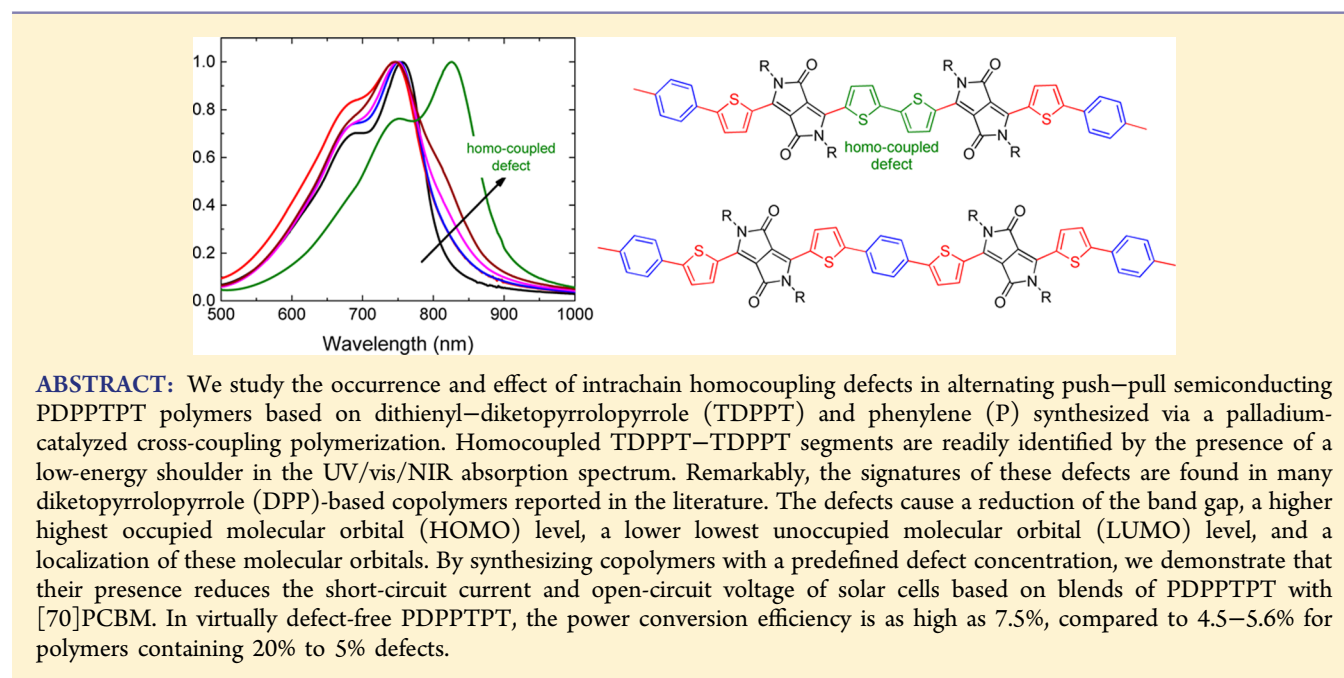


Homocoupling Defects in Diketopyrrolopyrrole-Based Copolymers and Their Effect on Photovoltaic Performance

Koen H. Hendriks, Weiwei Li, Gaël H. L. Heintges, Gijs W. P. van Pruissen, Martijn M. Wienk, and René A. J. Janssen*

Molecular Materials and Nanosystems, Institute for Complex Molecular Systems, Eindhoven University of Technology, P.O. Box 513, 5600 MB Eindhoven, The Netherlands

S Supporting Information



INTRODUCTION

In the quest for viable alternative energy sources, organic solar cells are making significant progress in terms of efficiency and reliability. Especially bulk heterojunction polymer/fullerene cells have received considerable attention, resulting in reported power conversion efficiencies (PCEs) up to 9.2% for single-junction devices and 10.6% for tandem cells.^{1,2} The design of new conjugated polymers for this application often relies on combining electron-rich donor (D) and electron-poor acceptor (A) moieties in an alternating push–pull polymer chain architecture. These donor–acceptor or push–pull polymers are commonly synthesized using a palladium-catalyzed (Stille or Suzuki) cross-coupling condensation polymerization reaction from complementary bifunctional monomers. The push–pull design allows control over the optical band gap and energy levels of the material by varying the nature of the alternating moieties incorporated in the chain and is the principal design motif for modern semiconducting polymers.

Besides the influence of the chemical nature of the components in the main chain and the resulting electronic and physical properties, various parameters govern organic solar cell performance.³ Some intrinsic factors are well-understood

such as energy losses and recombination processes,^{4,5} but also fullerene composition,⁶ molecular weight of the polymer,^{7,8} end group effects,⁹ and external impurities influence performance.^{10,11} Studies toward the influence of structural defects incorporated within the main chain of push–pull copolymers, such as homocoupling defects, however, have not been published to the best of our knowledge. This is, understandably, in part due to difficulties associated with identifying and characterizing main-chain defects in semiconducting polymers. In practice, it is implicitly assumed that the palladium-catalyzed reactions results in a perfect cross-coupling reaction. As we will demonstrate, homocoupling readily occurs when reaction conditions are not optimal and can have strong effects on the performance of the resulting polymer in a solar cell.

We focus our attention on polymers containing diketopyrrolopyrrole (DPP). The DPP unit is one of the electron-deficient groups that has been investigated extensively in recent years as a building block of semiconducting polymers. Owing to its electron deficiency, DPP is known for providing access to small

Received: June 3, 2014

Published: July 16, 2014

band gap polymers with high efficiencies in photovoltaic devices and ambipolar charge transport in field effect transistors.^{12–17} The UV/vis/NIR absorption of many high-performing DPP-based polymers published in literature is dominated by a $\pi \rightarrow \pi^*$ transition with charge transfer character and a distinct and steep onset at the optical band gap. Remarkably, in several published spectra, an additional shoulder at longer wavelengths can be observed. We assessed 131 recent publications on DPP-based copolymers and found that 38 reported absorption spectra of polymers with a distinct additional long-wavelength shoulder (see Table S1 of the Supporting Information for examples). In addition, 23 articles showed spectra with onsets of absorption at longer wavelengths than would be expected, but without direct evidence of a shoulder. At first glance the low-energy spectral feature might be attributed to aggregation of polymer chains, but a detailed assessment of the origin of this shoulder is usually absent. Owing to the multitude of DPP polymers published to date, it is possible to compare the spectra of some polymers that have the same conjugated backbone structure but have been prepared by different research groups. Even though the polymers can differ slightly in alkyl side-chain length, they inherently should have the same absorption spectrum and hence have identical optical band gaps. For instance, the onsets of absorption of PDPP2T-TT derivatives (i.e., where DPP alternates with 2,5-bis(thiophen-2-yl)thieno[3,2-*b*]thiophene, Figure 1) have been reported at 1.36,¹⁸ 1.34,¹⁹ 1.31,^{20,21}

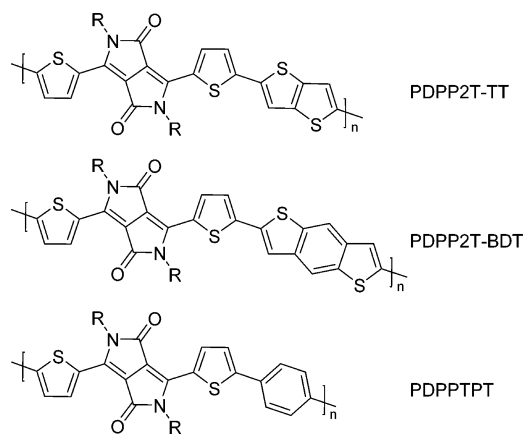


Figure 1. Structure of PDPP2T-TT, PDPP2T-BDT, and PDPPTPT.

1.23,²² and ~ 1.2 eV.²³ Even more outspoken differences occur for DPP polymers containing benzodithiophene (BDT). For PDPP2T-BDT with unsubstituted BDT units (Figure 1), an optical band gap of 1.31 eV²⁴ has been reported displaying a clear shoulder at lower energies, while from our own experience the onset is at 1.51 eV,²⁵ without the presence of a low-energy shoulder. Similarly, DPP-BDT polymers bearing alkoxy chains on the BDT have been reported with a very distinct shoulder^{26,27} or without.^{28,29} These remarkable differences have not yet been explained.

In this contribution we discuss a homocoupling defect that we have identified to occur while polymerizing the commonly used Br-TDPPT-Br monomer under suboptimal reaction conditions. The defect consists of a homocoupled DPPT-TDPP segment within the polymer chain and can be identified by a low-energy shoulder in UV/vis/NIR spectra. As a model system, PDPPTPT (Figure 1) is used as an easily accessible polymer to investigate the influence of these defects on the

photovoltaic performance.^{13,30} We compare PDPPTPT polymers that were synthesized with optimal and suboptimal reaction conditions and polymers that were synthesized with optimal conditions where a fixed amount of a Br-TDPPT-TDPPT-Br monomer was introduced in the reaction mixture to create a known amount of TT defects. The resulting defects can act as low-lying energy trap sites and effectively decrease the LUMO and increase the HOMO energy levels of the material. This reduces the photocurrent that can be obtained from solar cells when combined with [70]PCBM and leads to a significant reduction of the PCE. It is likely that the same type of shoulder found in some literature spectra of DPP-based copolymers also arises from homocoupled TT defects present in the polymer chain. We demonstrate the detrimental effect that a relatively small amount of defect can have on the photovoltaic performance and highlight the importance of carefully optimizing reaction conditions to obtain high-performing polymers.

RESULTS AND DISCUSSION

The PDPPTPT polymers were synthesized by a Suzuki polycondensation reaction of 3,6-bis(5-bromothiophen-2-yl)-2,5-bis(2-hexyldecyl)pyrrolo[3,4-*c*]pyrrole-1,4(2*H*,5*H*)-dione (Br-TDPPT-Br, **1**) and 1,4-benzenediboronic acid bis(pinacol) ester as shown in Scheme 1. A virtually defect-free PDPPTPT polymer (**P1**) was synthesized using an optimized 1:2 molar ratio of palladium and triphenylphosphine ligand. **P2** was synthesized using a 1:1 molar ratio of palladium to ligand, which represents suboptimal conditions. **P3**, **P4**, and **P5** were synthesized by introducing the homocoupled Br-TDPPT-TDPPT-Br (**2**) monomer in, respectively, 5, 10, and 20 mol % with respect to the Br-TDPPT-Br (**1**) monomer and using optimized reaction conditions. **P6** was obtained from condensation of **2** and 1,4-benzenediboronic acid bis(pinacol) ester. The formation of the homocoupled DPPT-TDPP defect when suboptimal reaction conditions are applied was verified with test reactions on **1** and phenylboronic acid pinacol ester (see Supporting Information, Figure S1).

The UV/vis/NIR spectra of the polymers in dilute chloroform solution and in thin films (Figure 2) show a clear trend in the onset of absorption for the polymers. While **P1** and **P6** have narrow absorption spectra in chloroform with a sharp onset at 1.57 and 1.42 eV, respectively, **P2–P5** have an onset in between these values, and the spectral shape is broadened and effectively a linear combination of the two parent absorption spectra **P1** and **P6**. For small amounts of incorporated TT defects (5%), this merely results in a low-energy shoulder that is hardly identified as an additional peak. **P2** shows a low-energy shoulder that exactly overlaps with the spectrum of **P3**, confirming the presence of TT homocoupling defects in **P2**. Also, a small blue shift of λ_{max} is observed, probably due to the lower molecular weight and presence of oligomeric species. These defects in **P2** have to originate from a side-reaction of the Br-TDPPT-Br monomers during the polymerization reaction because no Br-TDPPT-TDPPT-Br monomer was added. The spectral shape remains the same in the solid state, and the relative intensity of the long-wavelength shoulder in solution does not diminish at elevated temperatures, confirming that it is not an aggregation effect (Figure S2 in the Supporting Information). The differences between the spectra of **P1** and **P3–P5** also indicate that the former is virtually defect-free.

Gel permeation chromatography (GPC) analysis reveals that all polymers have high molecular weight; **P1** shows $M_n = 72$ kg

Scheme 1. Polymerization of P1–P6: (i) 1,4-phenylenebis(4,4,5,5-tetramethyl-1,3,2-dioxaborolane), Pd₂dba₃/PPh₃ (1:2), K₃PO₄, Aliquat 336, toluene, H₂O, 115 °C; (ii) 1,4-phenylenebis(4,4,5,5-tetramethyl-1,3,2-dioxaborolane), Pd₂dba₃/PPh₃ (1:1), K₃PO₄, Aliquat 336, toluene, H₂O, 115 °C. P3, *n* = 0.95, *m* = 0.05; P4, *n* = 0.90, *m* = 0.10; P5, *n* = 0.80, *m* = 0.20

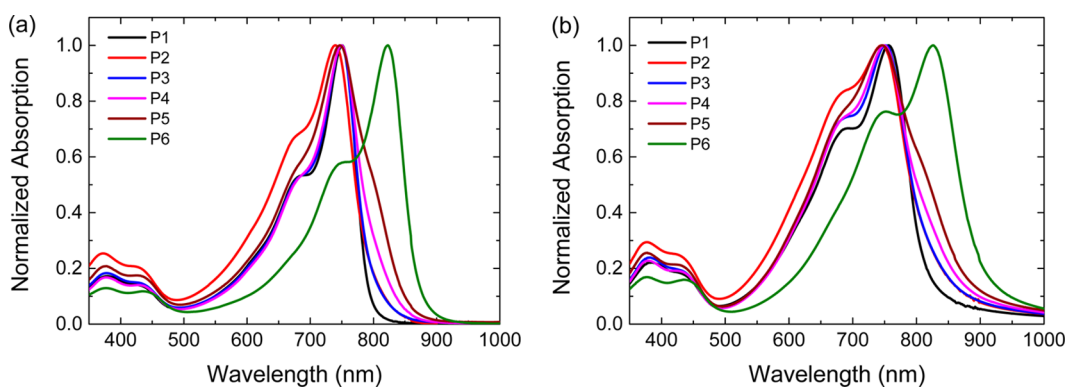
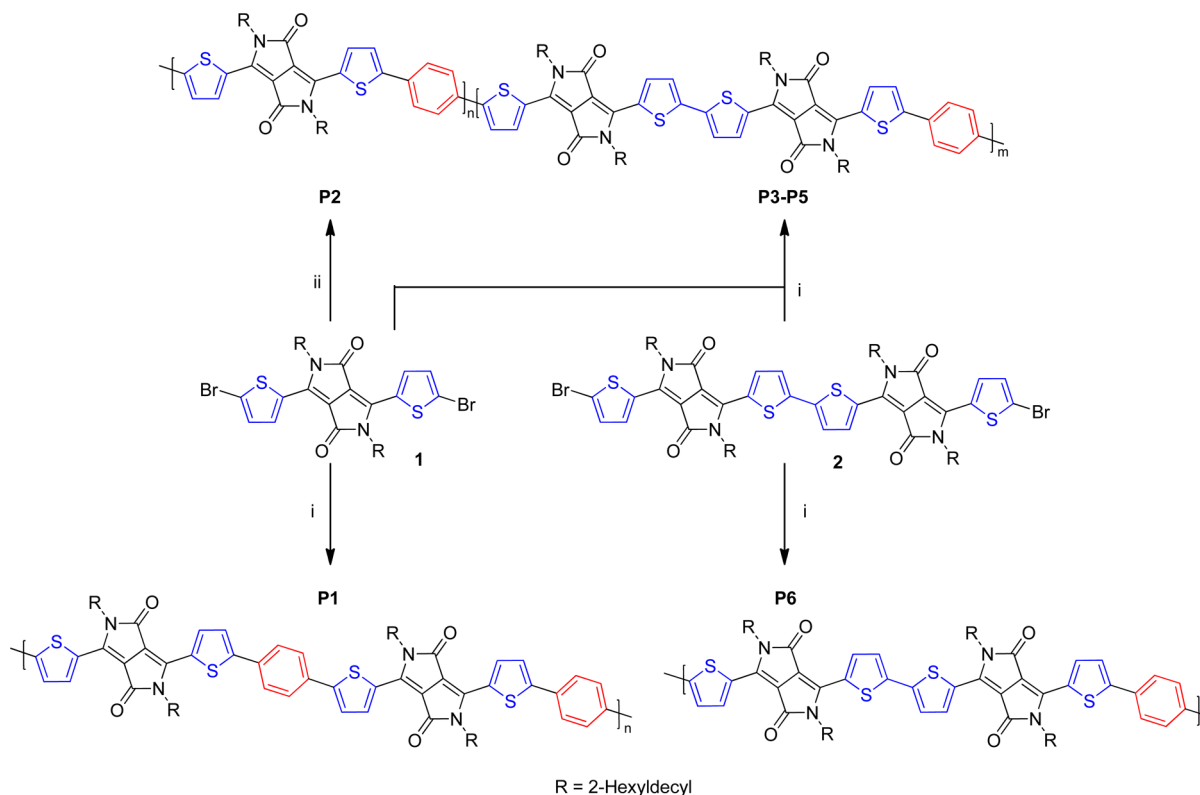


Figure 2. UV/vis/NIR absorption spectra of P1–P6: (a) in dilute chloroform solution and (b) in thin solid films.

Table 1. Molecular Weight, Optical Absorption, and Redox Potentials of PDPPTPT Polymers

	P1	P2	P3	P4	P5	P6
M_n (kg mol ⁻¹)	72	47	73	131	86	135 ^c
M_w (kg mol ⁻¹)	122	107	144	303	243	540 ^c
PDI	1.98	2.28	1.98	2.32	2.83	3.99 ^c
λ_{\max} (nm)	750	740	749	749	747	823
E_g^{sol} (eV)	1.57	1.48	1.48	1.47	1.45	1.42
E_g (eV)	1.53	1.40	1.40	1.39	1.38	1.37
E_{ox}^a (V)	0.56	0.55	0.54	0.50	0.48	0.46
E_{red}^a (V)	-1.44	-1.41	-1.42	-1.42	-1.39	-1.37
$E(\text{HOMO})^b$ (eV)	-5.79	-5.78	-5.77	-5.73	-5.71	-5.69
$E(\text{LUMO})^b$ (eV)	-3.79	-3.82	-3.81	-3.81	-3.84	-3.86

^aVersus Fc/Fc⁺. ^bDetermined using an energy of -5.23 eV for Fc/Fc⁺ vs vacuum. ^cSignal was in the exclusion limit of the column.

mol⁻¹. For the polymers **P3**–**P6** that were made with the same reaction conditions, similar or even higher molecular weights were measured (Table 1). The differences between the molecular weights of these batches could arise from small differences in the initial stoichiometry. **P2**, which was synthesized with the suboptimal 1:1 palladium/ligand catalyst system, clearly shows a lower M_n of 47 kg mol⁻¹. The lower molecular weight is most likely due to a resulting imbalance in monomer feed ratio inflicted by the homocoupling side-reaction or due to decomposition of the catalyst.³¹

Redox potentials and frontier orbital energy levels were estimated using cyclic voltammetry on thin films of the polymers in a liquid electrolyte (Figure S3 in the Supporting Information). Table 1 shows that the LUMO energy level for the polymers with defects (**P2**–**P6**) is lowered compared to **P1**, while the HOMO energy level is increased.

Density functional theory (DFT) calculations on B3LYP/6-31G(2d,p) level were performed for extended defect-free and defect-containing oligomers (Figure 3). In the DFT calculations

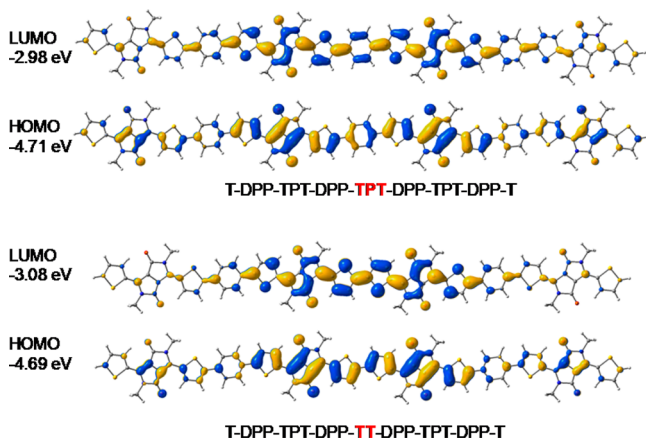


Figure 3. DFT frontier molecular orbitals for defect-free T-DPP-TPT-DPP-TPT-DPP-TPT-DPP-T (top) and defect-containing T-DPP-TPT-DPP-TT-DPP-TPT-DPP-T (bottom) oligomers of PDPPTPT.

the side-chains on the DPP unit were replaced by methyl groups and planarity was enforced between adjacent thiophene and phenyl rings. The calculated frontier orbitals (Figure 3) show that the TT defect results in a stronger localization of the HOMO and LUMO around the central TT defect compared to a central TPT unit. As a result the HOMO energy is raised from -4.71 to -4.69 eV and the LUMO energy is lowered

from -2.98 to -3.08 eV. Overall this leads to a reduced HOMO–LUMO energy gap difference of 0.12 eV, similar in magnitude to the experimental results.

The experimental and theoretical results show that a TT homocoupling defect in the alternating PDPPTPT polymer results in a lowering of the band gap and localization of the orbitals at the defect. As a consequence these TT homocoupling defects may act as a trap for excitons or charges.

To test the effect of the defects on device performance, solar cells were fabricated by combining the polymers **P1**–**P6** with [70]PCBM ([6,6]-phenyl-C₇₀-butyric acid methyl ester) as acceptor, sandwiched between a transparent ITO/PEDOT:PSS front contact and a reflective LiF/aluminum back contact. All polymer/[70]PCBM blend combinations were found to possess identical optimized processing conditions with a 1:2 weight ratio of polymer to fullerene and using 6 vol % *o*-DCB as additive in chloroform for spin coating. The current density–voltage (J – V) characteristics and external quantum efficiencies (EQEs) of the solar cells are displayed in Figure 4, and the cell parameters are summarized in Table 2. The defect-free material

Table 2. Solar Cell Characteristics for PDPPTPT Polymers

active layer	d (nm)	V_{oc} (V)	J_{sc}^a (mA/cm ²)	FF	EQE _{max}	PCE (%)
P1 /[70]PCBM	100	0.80	13.84	0.67	0.56	7.5
P2 /[70]PCBM	104	0.78	9.70	0.59	0.33	4.5
P3 /[70]PCBM	111	0.78	11.58	0.60	0.45	5.4
P4 /[70]PCBM	110	0.78	12.12	0.60	0.45	5.6
P5 /[70]PCBM	112	0.76	9.80	0.60	0.32	4.5
P6 /[70]PCBM	110	0.74	6.44	0.67	0.13	3.2

^aDetermined by integrating the EQE spectrum with the AM1.5G spectrum.

P1 has the highest performance with an open-circuit voltage (V_{oc}) of 0.80 V, a short-circuit current density (J_{sc}) of 13.84 mA cm⁻², and a fill factor (FF) of 0.67 under simulated AM1.5G conditions, resulting in a power conversion efficiency (PCE) of 7.5%. At the other extreme, **P6** shows a reduction in the V_{oc} of 60 mV, an identical fill factor, but a greatly reduced photocurrent of only 6.44 mA cm⁻², resulting in a PCE of only 3.2%.

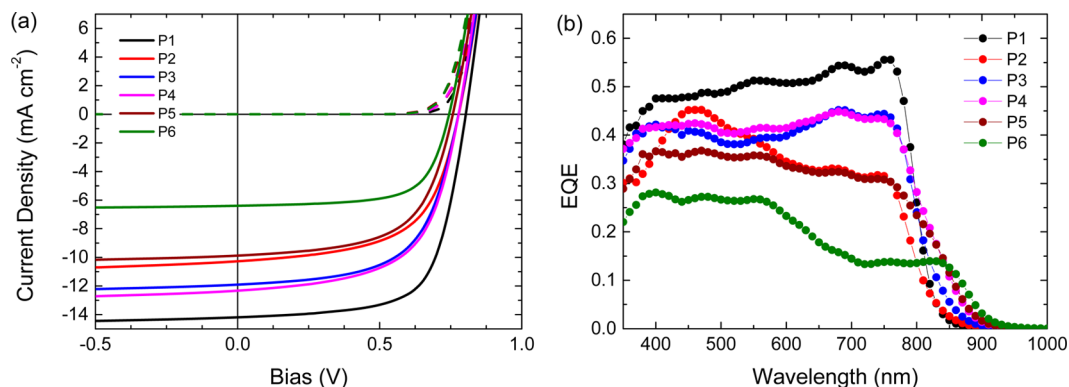


Figure 4. (a) J – V characteristics and (b) corresponding EQE spectra of solar cells from **P1**–**P6** blended with [70]PCBM.

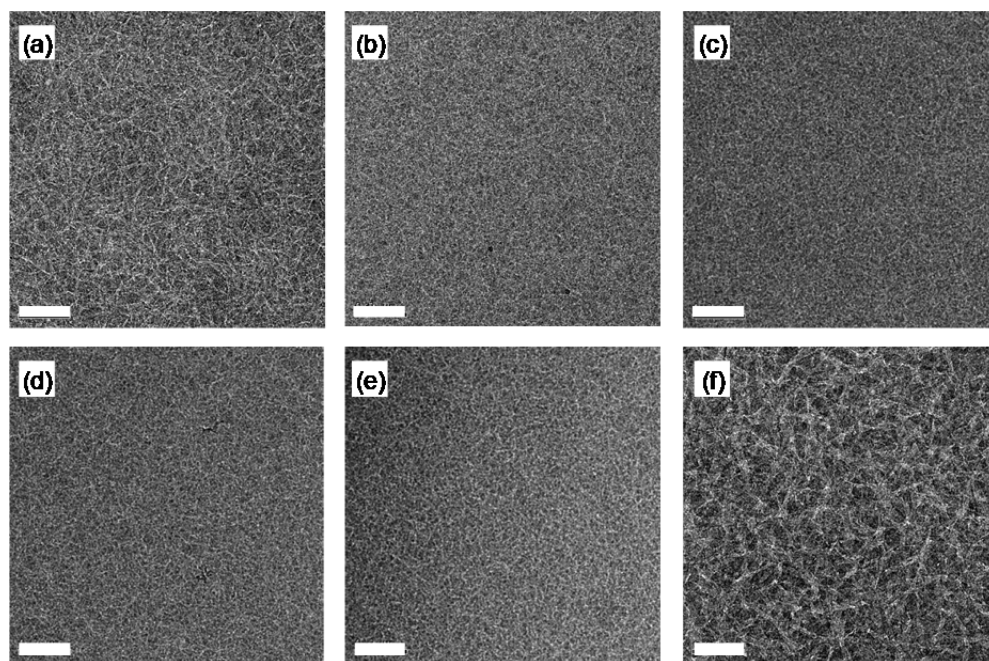


Figure 5. TEM images of active layers of (a) **P1**, (b) **P2**, (c) **P3**, (d) **P4**, (e) **P5**, and (f) **P6** with [70]PCBM. The scale bar is 200 nm.

The V_{oc} 's for **P2–P5** are in between those of **P1** and **P6** and reveal a trend that more defects lead to a lower V_{oc} . This is effectively due to the increase of the HOMO energy level of the polymer. The photocurrent follows a similar trend and shows that more homocoupling leads to a reduction of J_{sc} , except when comparing **P4** (10% defects) to **P3** (5% defects). In this case, the photocurrent of the polymer with more defects is slightly higher. We attribute this to the higher molecular weight of **P4**, and it shows that, although a material can have defects, it is still possible to obtain respectable PCEs. The virtually defect-free material **P1**, however, clearly outperforms all other PDPPTPT polymers, despite differences in molecular weight. For **P2** both the effects of a low molecular weight and the presence of defects drastically reduce the performance to PCE = 4.5%.

EQE spectra show a clear correlation between the contribution in the polymer region (600–900 nm) and the amount of homocoupling present in the material. In general, the EQE_{max} in the long-wavelength region is reduced from 0.56 for **P1** to 0.13 for **P6** when more TT defects are present. The decrease in EQE follows the trend of the polymers LUMO energy levels. We conjecture that the TT defects act as low-lying energy traps that inhibit formed excitons from splitting into free charges as the effective $LUMO_{donor} - LUMO_{acceptor}$ offset is reduced. The reduction potential of [70]PCBM at -1.09 V vs Fc/Fc^+ makes it that, going from **P1** to **P6**, the LUMO–LUMO offset drops below the 0.3 V difference that is generally considered as being necessary for electron transfer to occur. **P3** and **P4** have the same EQE_{max} and show the combined effects that a higher molecular weight increases EQE_{max} while more homocoupling defects decrease it again.

Transmission electron microscopy (TEM) images of the active layers show finely dispersed phase-separated morphologies for all blends (Figure 5). For **P1** and **P6**, fiber-like structures are observed that can help for efficient transport of free charges and result in good fill factors.²⁵ For **P2–P5** a slightly finer phase separation is observed and fill factors are less

because of the more mixed morphology or the presence of charge traps by the TT defects.

At this point the exact mechanism that is responsible for the homocoupling side-reaction in the synthesis of **P2** is not clear. We have observed this side-reaction in both Suzuki- and Stille-type polymerizations with the Br-TDPPT-Br monomer (see Supporting Information) and suspect that a palladium-catalyzed Ullmann type of homocoupling occurs yielding the DPP-TT-DPP defect and a $PdBr_2$ species.^{32,33} Subsequently this Pd(II) compound could be reduced by the consumption of boronic or stannyl monomers to obtain the active Pd(0) species again. The resulting imbalance in monomer feed ratio and presence of end-cappers then also explains the lower molecular weight of **P2**. For this example, the pathway to the side-reaction opens up when insufficient ligand is present and it can be suppressed by adding more. It is, however, clear that these defects should be avoided in order to obtain the highest performing materials by, for example, empirically optimizing the reaction conditions for every different polymerization.

CONCLUSION

A homocoupling defect was identified in DPP-based copolymers by the presence of a long-wavelength shoulder in the UV/vis/NIR absorption spectra. A series of PDPPTPT polymers with increasing amounts of homocoupled DPP-TT-DPP defects was synthesized to evaluate the influence of this defect on the photovoltaic performance. Polymers with defects show a large decrease in the photocurrent due to the localization of LUMO energy levels. This inhibits exciton separation, leading to a reduced photocurrent in solar cells based on defect-containing polymers. In addition, the higher lying HOMO energy level reduces the open-circuit voltage while the morphology becomes more finely separated, resulting in lower fill factors. The results show that these defects negatively influence the photovoltaic performance of these DPP-based polymers and should be minimized. Because similar low-energy shoulders are observed in many published absorption spectra of DPP copolymers synthesized by palladium-catalyzed Stille and

Suzuki cross-coupling reactions, it is reasonable to believe that these materials also suffer from homocoupling defects with the aforementioned consequences. As the cross-coupling reactions used here involve couplings among thiophene and phenylene units only, it is plausible that the homocoupling defects observed here are not limited to DPP-based polymers but commonly occur in semiconducting push–pull copolymers, but the extent of this remains to be established. At least for DPP-based polymers, these defects are easily detected by a low-energy shoulder or slant onset of the optical absorption spectrum.

■ ASSOCIATED CONTENT

● Supporting Information

Experimental details, synthesis and analysis of the monomers and polymers, literature examples of DPP polymer spectra with a long wavelength shoulder, validation of the homocoupling defect with suboptimal reaction conditions, additional figures, and the homocoupling example of PMDPP3T including solar cell data are described in the Supporting Information. This material is available free of charge via the Internet at <http://pubs.acs.org>.

■ AUTHOR INFORMATION

Corresponding Author

E-mail: r.a.janssen@tue.nl

Notes

The authors declare no competing financial interest.

■ ACKNOWLEDGMENTS

The work was performed in the framework of the Largecells and X10D projects that received funding from the European Commission's Seventh Framework Programme (Grant Agreement No. 261936 and No. 287818). The work was further supported by the "Europees Fonds voor Regionale Ontwikkeling" (EFRO) in the Interreg IV A project "Organext". The research forms part of the Solliance OPV programme and has received funding from the Ministry of Education, Culture and Science (Gravity program 024.001.035).

■ REFERENCES

- (1) He, Z. C.; Zhong, C. M.; Su, S. J.; Xu, M.; Wu, H. B.; Cao, Y. *Nat. Photonics* **2012**, *6*, 591–595.
- (2) You, J.; Dou, L.; Yoshimura, K.; Kato, T.; Ohya, K.; Moriarty, T.; Emery, K.; Chen, C.-C.; Gao, J.; Li, G.; Yang, Y. *Nat. Commun.* **2013**, *4*, 1446.
- (3) Janssen, R. A. J.; Nelson, J. *Adv. Mater.* **2013**, *25*, 1847–1858.
- (4) Blom, P. W. M.; Mihailetchi, V. D.; Koster, L. J. A.; Markov, D. E. *Adv. Mater.* **2007**, *19*, 1551–1566.
- (5) Koster, L. J. A.; Mihailetchi, V. D.; Blom, P. W. M. *Appl. Phys. Lett.* **2006**, *88*, 052104.
- (6) Street, R. A.; Davies, D.; Khlyabich, P. P.; Burkhart, B.; Thompson, B. C. *J. Am. Chem. Soc.* **2013**, *135*, 986–989.
- (7) Coffin, R. C.; Peet, J.; Rogers, J.; Bazan, G. C. *Nat. Chem.* **2009**, *1*, 657–661.
- (8) Wakim, S.; Beaupré, S.; Blouin, N.; Aich, B.-R.; Rodman, S.; Gaudiana, R.; Tao, Y.; Leclerc, M. *J. Mater. Chem.* **2009**, *19*, 5351–5358.
- (9) Park, J. K.; Jo, J.; Seo, J. H.; Park, Y. D.; Lee, K.; Heeger, A. J.; Bazan, G. C. *Adv. Mater.* **2011**, *23*, 2430–2435.
- (10) Nikiforov, M. P.; Lai, B.; Chen, W.; Chen, S.; Schaller, R. D.; Strzalka, J.; Maser, J.; Darling, S. B. *Energy Environ. Sci.* **2013**, *6*, 1513–1520.

- (11) Mateker, W. R.; Douglas, J. D.; Cabanetos, C.; Sachs-Quintana, I. T.; Bartelt, J. A.; Hoke, E. T.; El Labban, A.; Beaujuge, P.; Fréchet, J. M. J.; McGehee, M. D. *Energy Environ. Sci.* **2013**, *6*, 2529–2537.
- (12) Li, Y.; Sonar, P.; Murphy, L.; Honga, W. *Energy Environ. Sci.* **2013**, *6*, 1684–1710.
- (13) Hendriks, K. H.; Heintges, G. H. L.; Gevaerts, V. S.; Wienk, M. M.; Janssen, R. A. J. *Angew. Chem., Int. Ed.* **2013**, *52*, 8341–8344.
- (14) Bronstein, H.; Chen, Z.; Ashraf, R. S.; Zhang, W.; Du, J.; Durrant, J. R.; Tuladhar, P. S.; Song, K.; Watkins, S. E.; Geerts, Y.; Wienk, M. M.; Janssen, R. A. J.; Anthopoulos, T.; Siringhaus, H.; Heeney, M.; McCulloch, I. *J. Am. Chem. Soc.* **2011**, *133*, 3272–3275.
- (15) Dou, L.; Chang, H.-H.; Gao, J.; Chen, C.-C.; Jou, J.; Yang, Y. *Adv. Mater.* **2013**, *25*, 825–831.
- (16) Yiu, A. T.; Beaujuge, P. M.; Lee, O. P.; Woo, C. H.; Toney, M. F.; Fréchet, J. M. J. *J. Am. Chem. Soc.* **2012**, *134*, 2180–2185.
- (17) Ye, L.; Zhang, S.; Ma, W.; Fan, B.; Guo, X.; Huang, Y.; Ade, H.; Hou, J. *Adv. Mater.* **2012**, *24*, 6335–6341.
- (18) Zhang, G. B.; Fu, Y. Y.; Xie, Z. Y.; Zhang, Q. *Sol. Energy Mater. Sol. Cells* **2011**, *95*, 1168–1173.
- (19) Li, W.; Hendriks, K. H.; Roelofs, W. S. C.; Kim, Y.; Wienk, M. M.; Janssen, R. A. J. *Adv. Mater.* **2013**, *25*, 3182–3186.
- (20) Bijleveld, J. C.; Verstrijden, R. A. M.; Wienk, M. M.; Janssen, R. A. J. *J. Mater. Chem.* **2011**, *21*, 9224–9231.
- (21) Lee, J. S.; Son, S. K.; Song, S.; Kim, H.; Lee, D. R.; Kim, K.; Ko, M. J.; Choi, D. H.; Kim, B.; Cho, J. H. *Chem. Mater.* **2012**, *24*, 1316–1323.
- (22) Li, Y.; Singh, S. P.; Sonar, P. *Adv. Mater.* **2010**, *22*, 4862–4866.
- (23) Chen, Z. Y.; Lee, M. J.; Ashraf, R. S.; Gu, Y.; Albert-Seifried, S.; Nielsen, M. M.; Schroeder, B.; Anthopoulos, T. D.; Heeney, M.; McCulloch, I.; Siringhaus, H. *Adv. Mater.* **2012**, *24*, 647–652.
- (24) Jung, J. W.; Jo, J. W.; Liu, F.; Russell, T. P.; Jo, W. H. *Chem. Commun.* **2012**, *48*, 6933–6935.
- (25) Li, W. W.; Hendriks, K. H.; Furlan, A.; Roelofs, W. S. C.; Wienk, M. M.; Janssen, R. A. J. *J. Am. Chem. Soc.* **2013**, *135*, 18942–18948.
- (26) Huo, L.; Hou, J.; Chen, H.-Y.; Zhang, S.; Jiang, Y.; Chen, T. L.; Yang, Y. *Macromolecules* **2009**, *42*, 6564–6571.
- (27) Zhang, S.; Ye, L.; Wang, Q.; Li, Z.; Guo, X.; Huo, L.; Fan, H.; Hou, J. *J. Phys. Chem. C* **2013**, *117*, 9550–9557.
- (28) Tandy, K.; Dutta, G. K.; Zhang, Y.; Venkatramiah, N.; Aljada, M.; Burn, P. L.; Meredith, P.; Namdas, E. B.; Patil, S. *Org. Electron.* **2012**, *13*, 1981–1988.
- (29) Wang, Y.; Yang, F.; Liu, Y.; Peng, R.; Chen, S.; Ge, Z. *Macromolecules* **2013**, *46*, 1368–1375.
- (30) Bijleveld, J. C.; Gevaerts, V. S.; Di Nuzzo, D.; Turbiez, M.; Mathijssen, S. G. J.; de Leeuw, D. M.; Wienk, M. M.; Janssen, R. A. J. *Adv. Mater.* **2010**, *22*, E242–E246.
- (31) Bao, Z.; Chan, W. K.; Yu, L. *J. Am. Chem. Soc.* **1995**, *117*, 12426–12435.
- (32) Hassan, J.; Penalva, V.; Lavenot, L.; Gozzi, C.; Lemaire, M. *Tetrahedron* **1998**, *54*, 13793–13804.
- (33) Hennings, D. D.; Iwama, T.; Rawal, V. H. *Org. Lett.* **1999**, *1*, 1205–1208.